The microstructure and electrochemical properties of Al/Pb-Ag anode for zinc electrowining[1]

Zhang Yongchun[a*], Guo Zhongcheng [b]

[a]Department of Mechanical Engineering, Baoji Uniyersity of Arts and Science, Shaanxi Baoji 721013, China

[b]Kunming Hendera Science and Technology Co. Ltd, Kunming 650106, China

Keywords: galvanostatic deposition; energy consumption; anode potential; zinc electrowinning

Abstract: Al/Pb-0.8%Ag and Al/Pb-0.75%Ag-0.03%Co anodes were successfully obtained by electrodeposition from methanesulfonic acid. The relation of silver content(y/m%×10^4) in Pb-Ag coatings and Ag^+ concentration(x/mgdm^{-3}) of electrolyte was $y=-60.25+0.92x$. The results of anode polarization curves and Time-Potential curves showed Al/Pb-0.75%Ag-0.03%Co had the lowest energy consumption and anode potential during zinc electrowinning.

Introduction

Recent years have seen extensive studies of aluminum substrate composite anodes used in zinc electrowinning, as seen in[1-3] and reference therein. The Al/α-PbO_2, Al/β-PbO_2 and Al/Pb-PANI-WC composite anodes are relatively low in cost and anode potential during zinc electrowinning for their coatings and substrate, but the service time of them are not satisfied due to the bindingforce between aluminum substrates and α,β-PbO_2 coating, and higher corrosion rate of Pb-PANI-WC coating during zinc electrowinning. Lead anodes with a silver content of about 0.5%-1% are used in zinc electrowinning. To save silver it's suggested that a Pb-Ag alloy with about 0.45-1%Ag and a thickness of 100-200μm as the active anode surface on a lead anode will suffice. Deposition of Pb-Ag alloys from cyanide-free electrolytes was also investigated. Electrolytes using potassium hexacyanoferrate(Π), K4Fe(CN)6, and polyethylenepolyamines as complexing agents were tested[4,5]. In this communication, we report the preparation, properties and microstructure of Al/Pb-Ag and Al/Pb-Ag-Co anodes with unusual characteristics. Pb-Ag and Pb-Ag-Co coatings have different microstructure and its oxygen evolution potential and energy consumption are lower than conventional Pb-Ag anode.

Experimental details

The electrolytes contained 0.5-1.2mol dm^{-3} lead methanesulfonate, 0.5-2mmol dm^{-3} silver methanesulfonate, 0-20mmol dm^{-3} cobalt methanesulfonate, 0.5-2mol dm^{-3} methanesulfonate acid, 10-30μmol dm^{-3} polyvinylpyrrolidone, 0.15-0.45mol dm^{-3} sulfourea. All chemicals were analytical reagent grade from Aldrich and Fisher. All solutions were prepared with ultra-pure water. Electrodeposition was conducted at pH values in the 1.5-2 range, at a cathodic current density of J=1 Adm^{-2}, and with mechanical bubbling for 24 h at 40 °C.

The aluminum substrates were pretreated by buffing(mechanical buffing with fibre grinding wheel), degreasing (soak in fatty alcohol-polyoxyethylene ether degreaser at 40℃ for 4-12h), caustic wash (soak in 0.3mol dm^{-3}, solution at 20-40℃ for 120-180 seconds), acid pickling(0.4mol dem-3 sulfuric acid at 20-40℃ for 10-30 seconds), zinc immersion (soak in 0.3mol dm^{-3}, 0.25mol dm^{-3}, 3mmol dm^{-3} sodium potassium tartrate, 0.5mmol dm^{-3} iron chloride hexahydrate solution at 20-40℃ for 60 seconds), acid pickling(3-10s), zinc immersion (at 20-40℃ for 50 seconds) and nickel electroplating for 1 minute.

All electrochemical measurements were made with electrochemical workstation (CHI760C) with three electrode systems. A following set-up was used: $ZnSO_4$-H_2SO_4 system, 0.9mol dm^{-3} Zn^{2+}, 1mol dm^{-3} sulfuric acid and temperature (35 °C). The counter electrode was a platinum plate and the reference electrode was MSE with a potential of E_{MSE}= +0.64 V. The three anodes were used as working electrodes after 24h of anodic polarization. Microstructure characterisation were carried out using a scanning electroscopy (Sirion200SEM, FEI), a 30ke accelerate voltage and 1 minutes collection time.

Result and discussion

Pb-0.8%Ag layer was deposited from a solution containing 1mol dm^{-3} lead methanesulfonate, 1.4mmol dm^{-3} silver methanesulfonate, 1.2mol dm^{-3} methanesulfonate acid, 20μmol dm^{-3} polyvinylpyrrolidone, 0.3mol dm^{-3} sulfourea. Pb-0.75%Ag-0.03%Co layer was deposited from a solution containing 1mol dm^{-3} lead methanesulfonate, 0.5-2mmol dm^{-3} silver methanesulfonate, 1.2mol dm^{-3} methanesulfonate acid, 0-20mmol dm^{-3} cobalt methanesulfonate, 20μmol dm^{-3} polyvinylpyrrolidone, 0.3mol dm^{-3} sulfourea.

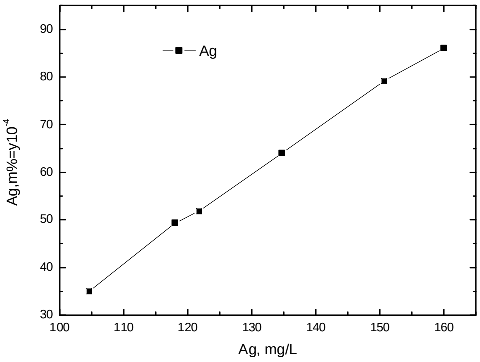

Fig.1The influence of Ag$^+$ concentration of electrolyte on Ag content of Pb-Ag composite coatings

Fig.1 reports the influence of Ag$^+$ concentration of electrolyte on Ag content of Pb-Ag composite coatings. It's found that Ag$^+$ of electrolyte need supplement pure hour. The relation of Ag content of Pb-Ag coatings and Ag+ concentration of electrolyte is equation (1):

$$y = -60.25 + 0.92x, \quad (1)$$

There y represents Ag content of Pb-Ag coatings and x represents Ag$^+$ concentration of electrolyte. The error limit of equation (1) versus the true value of Ag content(m%) of Pb-Ag coatings is ±0.03.

Fig.2 presents the anode polarization curves for the Tafel analysis of Pb-0.8%Ag, Al/Pb-0.8%Ag and Al/Pb-0.75%Ag-0.03%Co anodes carried out a zinc sulphate electrolyte. The parameters of oxygen evolution dynamics are listed in Table 1.

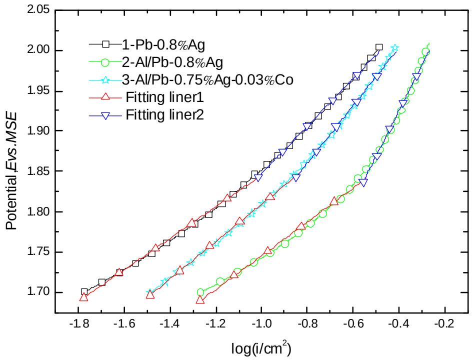

Fig.2 Tafel analysis of Pb-0.8%Ag, Al/Pb-0.8%Ag and Al/Pb-0.75%Ag-0.03%Co anodes

Table 1 OER dynamic parameters of Pb-0.8%Ag, Al/Pb-0.8%Ag and Al/Pb-0.75%Ag-0.03%Co anodes

Anodes	Fitting line 1		Fitting line 2		$i^0/(Acm^{-2})$		$h_a(i=0.05Acm^{-2})/V$
	a	b	a	b	i_1^0	i_2^0	
Pb-0.8%Ag	0.718	0.195	0.898	0.293	8.13×10^{-5}	8.71×10^{-4}	0.464
Al/Pb-0.8%Ag	0.713	0.209	0.909	0.566	3.89×10^{-4}	2.45×10^{-2}	0.441
Al/Pb-0.75%Ag-0.03%Co	0.709	0.232	0.904	0.357	8.71×10^{-4}	2.95×10^{-3}	0.407

The anodic polarization curve for Tafel analysis was corrected by using the following formula [6]:

$$E_a = E_{appl} - iR_s, \qquad (2)$$

There E_a is the real potential value of OER, E_{appl} is the applied potential, i is the faradaic current, and R_s is the uncompensated electrolyte resistance[7]. Fig. 2 shows the iR-corrected Tafel lines of Pb-0.8%Ag, Al/Pb-0.8%Ag and Al/Pb-0.75%Ag-0.03%Co anodes on stable anodic layers after 24 h of anodic polarization. All lines presented a double-slope behavior. Based on the OER mechanism, the double-slope values and potential intercepts of the two lines were separately analyzed by using Origin software. The over-potential h under specific current was calculated with Tafel based on the following formula [6]:

$$\eta = a + b\log i, \qquad (3)$$

where a and b are constants, i is the electrode surface current density, and h is the OER overpotential. a and b are obtained through liner fitting of the plot h versus $\log i$, where $a = a_i - E$. Comparing the Tafel and the Butler–Volmer formulas in the high anodic polarization region, we can express the exchange current density i^0 as follows:

$$\log i^0 = -\frac{a}{b}, \tag{4}$$

where i^0 is the exchange current density, i is the experiment current, a_i is the intercept value obtained with Origin, and E is the standard potential. Generally, the values of i^0 for OER are negligibly small and often considered meaningless in evaluating the electrocatalytic activity of anode materials. As a result, the OER overpotentials h are identified as one of the major criteria. The h of Al/Pb-0.75%Ag-0.03%Co and Al/Pb-0.8%Ag anodes lower than Pb-0.8%Ag anode which indicates that the two anodic layers are preferable to OER. In addition, Al/Pb-0.75%Ag-0.03%Co and Al/Pb-0.8%Ag anodes present a higher b_1 and b_2, probably because of the impeded mass and charge transfer in the micropores and its microstructure that is prone to O_2 evolution [8-9].

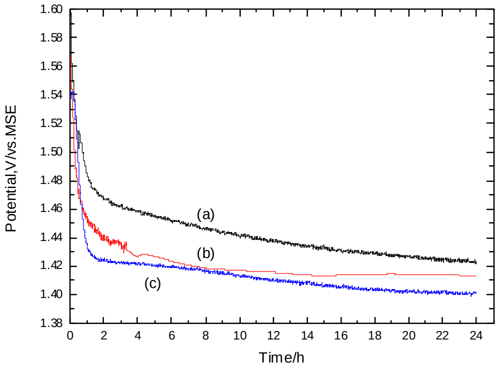

Fig.3 Time-Potential curves carried out an electrolyte containing 0.9mol $dm^{-3}Zn^{2+}$ and 1.5mol $dm^{-3}H_2SO_4$. (a) Conventional Pb-0.8%Ag anode, (b) Al/Pb-0.8%Ag anode (c)Al/Pb-0.75%Ag-0.03%Co anode

Fig.3 shows the anode potentials with time for the zinc electrowinning tested. Pb-0.8%Ag, Al/Pb-0.8%Ag and Al/Pb-0.75%Ag-0.03%Co anodes have a high anode potential and decrease sharply at the first beginning zinc electrowinning, which is due to the dissolution of non-conducting phase of PbO and PbO_2. Then the anode potentials decrease slowly which is due to the intermediate product of $PbSO_4$ and PbO_2. After 22h of zinc electrowinning, the anode potentials remained constant, showing that the three anodic layers mainly composed of β-PbO_2[10],. Compared with Pb-0.8%Ag anode, the anode potential of Al/Pb-0.8%Ag is decreased by 10mv and Al/Pb-0.75%Ag-0.03%Co anode is decreased by 22mv.

3.4 Mechanism of Co on activity

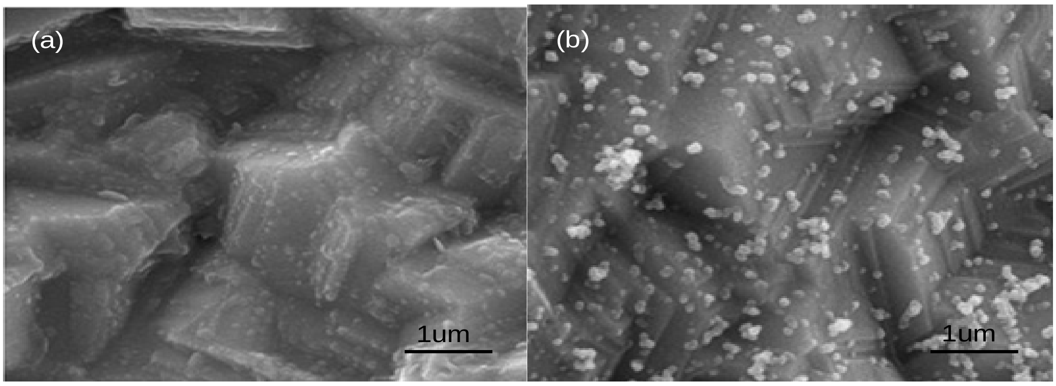

Fig.4 Fruit surface microstructure. (a) Al/Pb-0.8%Ag anode (b)Al/Pb-0.75%Ag-0.03%Co anode

Fig.4 shows the fruit surface microstructure of Al/Pb-0.8%Ag(a) and Al/Pb-0.75%Ag-0.03%Co(b) anodes. As shown in Figs. 4a and 4b, the size of lead crystals on the Al/Pb-0.75%Ag-0.03%Co anode is smaller than that of crystals on the Al/Pb-0.8%Ag anode. The silver on the fruit surface of the Al/Pb-0.75%Ag-0.03%Co anode is bulbiformed, and the silver crystals are attached to the surface of the lead composite coating (Fig.4a). However, the silver on the fruit surface of the Al/Pb-0.8%Ag anode has an elliptical shape and the silver crystals are covered with lead (Fig.4b). The different crystal sizes of lead, as well as the shape and existing way of silver, are probably caused by the existence of cobalt in the Pb-0.75%Ag-0.03%Co composite coating.

Conclusions

Al/Pb-0.8%Ag and Al/Pb-0.75%Ag-0.03%Co anodes have obtained by non-cyanide electrodeposition from electrolyte. The results of tafel and time-potential analysis show that Al/Pb-0.8%Ag and Al/Pb-0.75%Ag-0.03%Co anodes have lower anode potential as compared to conventional Pb-0.8%Ag anode for zinc electrowinning. The catalytic processes of Co on the surface of the Al/Pb-0.75%Ag-0.03%Co anode during zinc electrowinning can be described by the following reaction: $Co \rightarrow Co^{2+} \rightarrow Co^{3+}$.

Acknowledgment

Financial supports for this work from the Baoji science and technology project(14GYGG-2-4)

References

1. B. Chen, Z. Guo, H. Huang, et al. Effect of the current density on electrodepositing alpha-lead dioxide coating on aluminum substrate[J]. Acta Metallurgica Sinica, 2009, 22(5):373–382. Chen Z, Wu J, Guo Z C, et al. Influence of Fluoride Ion on the Electrochemical Properties of Al/β-PbO2 Electrode[J]. Advanced Materials Research, 490-495(2012)3160-3166.
2. R. Xu, L. Huang, J. Zhou, et al. Effects of tungsten carbide on electrochemical properties and microstructural features of Al/Pb-PANI-WC composite inert anodes used in zinc electrowinning[J]. Hydrometallurgy, 2012, 125(8)(2012)8–15.
3. Y. Zhang, R. Hu, R. Xiang. Electroplating Handbook. National defense industry press[M]. 2011, 389-394.
4. G. I. Ostapenko. Electrochemical reactions at a copper electrode in copper-conducting solid electrolytes[J]. Russian Journal of Electrochemistry, 43(4)(2007)470-474.
5. Y. Lai, Y. Li, L. Jiang, et al. Electrochemical behaviors of co-deposited Pb/Pb–MnO 2 composite anode in sulfuric acid solution – Tafel and EIS investigations[J]. Journal of Electroanalytical Chemistry, 671(5)(2012)16–23.
6. Franco Silva D V, Da Jardim L M, et al. Influence of the electrolyte composition on the kinetics of the oxygen evolution reaction and ozone production processes[J]. Journal of the Brazilian Chemical Society, 17(4)(2006)446-757.
7. L. M. D. Silva, L. A .D. Faria, J. F. C. Boodts. Electrochemical ozone production: influence of the supporting electrolyte on kinetics and current efficiency[J]. Electrochimica Acta, 2003, 48(2003)699–709.
8. R. Kötz, S. Stucki. Ozone and oxygen evolution on PbO2 electrodes in acid solution[J]. Journal of Electroanalytical Chemistry & Interfacial Electrochemistry, 228(1)(1987)407–415.
    a) Sirés, C. T. J. Low, C. Ponce-de-León, et al. The deposition of nanostructured β-PbO2

coatings from aqueous methanesulfonic acid for the electrochemical oxidation of organic pollutants[J]. Electrochemistry Communications, 12(2010)70–74.

9. E. K. Alamdari, D. Darvishi, M. S. Khoshkhoo, et al. On the way to develop co-containing lead anodes for zinc electrowinning[J]. Hydrometallurgy, 119 (5) (2012)77–86.